

I Neutron Scattering

I.1 Basic Concepts

Ferenc Mezei

I.1.1 INTRODUCTION

The observation of scattering of radiation is one of the most common ways to see objects in everyday life: The light from the sun or a lamp falls on the objects around us and is partially absorbed and partially scattered. It is the observation of the scattered radiation by the eyes that allows us to “see” things around us, primarily the surface of the objects. Some materials such as glasses, gases, and many liquids neither scatter nor absorb much of light, so they are largely transparent or nearly invisible. The partial reflection of light on glass surfaces is also a form of scattering, and analogous processes with neutrons are widely used to study optically flat interfaces.

The way eyes and similarly operating cameras detect and process scattered light is called optical imaging, which is based on the capability to have focusing devices (lenses) with a reasonably large angular acceptance, which is related to the power to deviate the radiation by a substantial angle in the range of 10° or more. This is not the only way to extract information from scattered radiation. The information carried by the modified sound reaching us from objects behind obstacles or from moving objects gives a vague and limited idea of what can be inferred from the observation of more subtle properties of scattered radiation without the capability of image formation. The example of bats using sonar-like technology by capturing ultrasound scattered by flying insects is a particularly telling example.

The basic physical properties of the radiation determine the features of the objects we can observe. Light has a wavelength λ in the range of a few tenths of a micron, and this leads to an unavoidable lower limit of geometrical details, which can be observed by using light. Although the optical capabilities of our eyes cannot fully exploit these confines, with the help of microscopes we can look for finer details down to the limit set by the wavelength of the light radiation used. Other limit is set by the capability of the radiation to make its way inside the materials observed. Light is absorbed in most materials within a very short distance, so the scattered radiation

2 Basic Concepts

originates from the immediate vicinity of the surface of the objects; hence, it is not adequate to gain information from the inside of such materials.

X-rays, which essentially are very short wavelength light, have wavelength in the Å range ($1 \text{ Å} = 0.1 \text{ nm}$), just as the distance between atoms in chemical bonds or in condensed matter. Therefore, they can offer the capability to observe the atomic structure of matter, for which purpose X-ray diffraction is the oldest and most common method of exploration. Here we already meet a major difference compared to vision based on light: there is no way to directly observe images. This is due, on the one hand, to the fact that we do not know materials that could be used to produce X-ray optical devices, which could deviate this radiation by a substantial angle in the range of several degrees. (Even if this would not be the case, it would still be of quite some challenge to build optical devices with stability and precision of an Å or so. This, however, could be ingeniously achieved with scanning tunneling microscopes, atomic force microscopes, and similar devices for the study of surfaces with atomic resolution!) For this reason, the actual three-dimensional atomic image building has to be achieved by another way: by complex mathematical reconstruction from the scattering patterns arising due to interference of the radiation scattered on various atoms, more or less close to each other in the sample. With the advent of very intense future X-ray sources, such as free electron lasers, it is hoped that such reconstruction of the 3D image of the atoms will also become possible for samples consisting of a single large molecule.

Neutron radiation can also provide us with a probe with wavelength in the Å range, and thus make possible to observe atomic structures similarly to X-rays. Indeed, this has become a standard tool in the study of condensed matter since the groundbreaking discoveries by C. Shull and coworkers around 1950. In this type of research, the scarcer and more expensive neutron radiation is less commonly used than one or the other forms of X-ray sources, including tabletop laboratory equipment. However, neutrons offer a number of special capabilities for collecting information fully inaccessible to X-rays: (a) neutrons can observe light atoms (including hydrogen) in the presence of heavier ones; (b) neutrons can penetrate inside complex equipment for *in situ* studies or inside bulky samples to reveal structures far from the surface; and (c) neutrons allow to mark selected atoms within a given species in the sample by isotopic replacement. The large difference in the neutron scattering characteristics between hydrogen and deuterium is of particular importance in the study of biological matter.

Radiation in general is characterized not only by its wavelength, but also by its frequency. Here there is another very important difference between neutrons and X-rays. The relation between wavelength λ and frequency f for X-rays is given as

$$f = c/\lambda,$$

where c is the velocity of light, $299,792,458 \text{ m/s}$, and for radiation with wavelength of 1 Å we have $f \cong 3 \times 10^{18} \text{ Hz}$. This is a very high frequency that corresponds to 12.5 keV energy or to the thermal energy $k_{\text{B}}T$ at a temperature of about 150 million K.

In contrast to X-rays, the neutron velocity v depends on the wavelength, according to the de Broglie relation

$$mv = 2\pi\hbar/\lambda, \quad (\text{I.1.1})$$

where m is the neutron mass and \hbar is the Planck constant. With this, the frequency f of the neutron radiation becomes

$$f = v/\lambda = \frac{2\pi\hbar}{m\lambda^2}, \quad (\text{I.1.2})$$

which for $\lambda = 1 \text{ \AA}$ gives $f \cong 1.97 \times 10^{13}$ Hz, corresponding to 81.8 meV or to the thermal energy at 950K.

The huge difference between the frequencies of X-ray and neutron radiations of the wavelength comparable to atomic radii has the major consequence that atomic motions in materials under everyday conditions can be readily traced by neutron radiation, and this can be only partially accomplished by X-rays, or by any other radiation known to us, for the same matter. The scattering of radiation on atoms in motion is a quantum mechanical process, in which quanta of energy $\hbar\omega$ can be exchanged between the radiation and the sample, where $f \equiv 2\pi/\omega$ is a characteristic frequency of the motion of the atoms in the sample. In such a so-called “inelastic scattering” process, the energy of the scattered radiation is different from the incoming one by the amount $\hbar\omega$: either larger (called “energy gain scattering”) or lower (called “energy loss scattering”).

The motion of atoms in matter under ordinary conditions is thermally excited, and the possible frequencies of various kinds (“modes”) of atomic motions in condensed matter range from essentially 0 (e.g., sound waves of a few tens or hundreds of Hz) to the equivalent of thermal energies at which the materials disintegrate, for example, a solid melts or a liquid evaporates. For ordinary materials, this corresponds to a few hundred to 1000K, pretty close to the equivalent of the energy of neutrons with $\lambda = 1 \text{ \AA}$ wavelength. Therefore, we conclude that in ordinary matter inelastic scattering processes of this kind change the neutron energy by a substantial, easily detectable amount, while for X-rays with similar wavelength the change is in the range of a part in a million. This difference becomes decisive for the study of slower atomic or molecular motions. At the end, inelastic neutron scattering allows us to explore microscopic process in the time domain of 10^{-15} to 10^{-6} s (i.e., energies from neV to eV), while inelastic X-ray scattering cannot access times longer than 10^{-11} s (energies less than about a few tenths of a meV). This capability of exploring slow processes, together with its high sensitivity to look at hydrogen atoms, makes neutrons one of the particularly valuable tools for the microscopic investigation of soft matter.

It is worth emphasizing that the important feature of these radiations in the study of condensed matter is the direct exploration of the microscopic and nanoscopic time and length domains in both of its dimensions. This is made possible by being able to detect appropriate changes in frequency in the scattering process for radiation with wavelength comparable to the size of atoms or molecules. This offers invaluable

4 Basic Concepts

additional insight into information on dynamics one can obtain by macroscopic spectroscopies, such as light scattering, dielectric response, and so on, exploring the average behavior of bulk matter, or by local probes, such as NMR, μ SR, and so on, which directly test single atoms. The understanding of cooperative, collective aspects of the motion of atoms and molecules requires the additional dimension offered by neutron and to a lesser extent X-ray radiation: to directly observe the evolution of microscopic motion in the domain between the local atomic and the bulk macroscopic length scales.

Neutrons are particularly formidable microscopic probes of magnetism, due to their magnetic moment that can scrutinize the internal magnetic fields \mathbf{B} on the atomic level inside materials. Magnetism is less common in soft matter; however, the sizable magnetic moment of neutrons—in contrast to their lack of electric charge—is a valuable additional experimental handle one can also make unique use of in experimental exploration of nonmagnetic materials, and as such also of prime importance in soft matter studies.

I.1.2 RADIATION OF PARTICLES AND WAVES

The quantum mechanical duality between the particle and wave aspects of radiations used in scattering experiments is of fundamental importance in the practice of neutron scattering. As a rule of thumb, any radiation (even familiar waves as light) behaves as an ensemble of point-like classical particles when propagating between obstacles (structures) very large compared to its wavelength. In contrast, when the structure has details comparable in size to the wavelength of the radiation, wave propagation needs to be considered, with all the complexities of interference effects.

The physical reason for this behavior is that if optical path differences in wave propagation span a range much larger than the wavelength, interference effects will occur with a wide spread of phase differences in excess of 2π . Therefore, these effects, the single experimental signature of wave propagation, will average to zero, and the wave looks like an ensemble of classical point-like particles following uniquely determined, precise trajectories, for example, as in geometrical optics.

A more practical and quantitative criterion for particle versus wave behavior can be formulated by considering the way radiation is collimated for the purposes of scattering experiments. For neutron beams, we have typically about 10^6 – 10^8 particles/cm²/s. If we would need to study a sample, for example, a crystalline grain of say 0.1 mm diameter, this would mean mere 100–10000 neutron/s impinging on the sample, far from enough for a reasonable scattering experiment. This illustrates the point that neutron scattering is an “intensity-limited” technique and we need most often to use beam cross sections and sample areas in the range of cm² or more. With such sample size, in order to achieve a well-defined beam direction a few meter flight path is quite common. How an obstacle of a $d = 1$ cm diameter hole in $L = 10$ m distance relates to the wavelength of the radiation can be evaluated by considering the possible path differences between wave/particle paths from one point to another along the beam propagation. Figure I.1.1 illustrates possible paths of beam

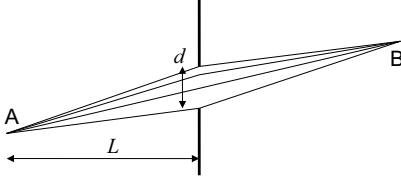


Figure I.1.1 Potential optical paths for wave propagation from point A to point B through a diaphragm as obstacle.

propagation defined by a diaphragm as obstacle. The maximum possible difference in optical path lengths is given by

$$\delta = 2 \left(\sqrt{L^2 + (d/2)^2} - L \right) \cong \frac{d^2}{4L}. \quad (\text{I.1.3})$$

With $L \sim 10$ m and $d \sim 1$ cm, we get $\delta \sim 0.0025$ mm = 2500 nm, that is, about four orders of magnitude larger than the neutron wavelength. Thus, here the neutron can be considered as a classical point-like particle. For visible light, however, with $\lambda \sim 500$ nm one would be better advised to use wave mechanics to precisely evaluate an experiment, as it was well known nearly 200 years ago. At synchrotron X-ray sources, the typical beam diameter $d \sim 0.1$ mm, that is, we have $\delta \sim 2.5$ Å, which is indeed comparable to the wavelength of the radiation we are interested in.

Eq. (I.1.3) also implies that if we consider the propagation of neutrons inside materials, where the “obstacle” structure means atoms or molecules at distances d from each other in the range of a few Å or nm, we will always encounter wave behavior, independently of the value of L (which practically cannot be less than atomic distances). In practical terms, this leads to the basic rule of neutron scattering experimentation (and implies a great practical simplification of data reduction): the beam propagation in the spectrometers outside materials can be exactly described by classical mechanics of point-like particles. This is in contrast to synchrotron X-ray scattering, which fact is commonly and rather imprecisely referred to by calling synchrotron X-rays “coherent” and neutrons “incoherent” radiation. In actual fact, there is no difference in the coherence of these radiations as far as their interaction with the samples is concerned; the difference is instead in their interaction with the spectrometers operating with very different beam cross sections.

This classical particle (“incoherent”) behavior of neutron beams as shaped and observed in scattering instruments paradoxically leads to a simplification of the description of the scattering process of neutrons on the atomic scale details in materials. Since the state of a classical particle impinging on a scattering objects can be described by a well-defined velocity vector \vec{v} , it will be characterized as a wave by a single, well-defined wavelength λ , as given by eq. (I.1.1), and the corresponding exact plane wave will thus be given as

$$\phi = e^{i(\vec{k}\vec{r} - \omega t + \phi_0)}, \quad (\text{I.1.4})$$

where the wave vector \vec{k} is defined as $\vec{k} = m\vec{v}/\hbar$ (i.e., the absolute value of \vec{k} equals $2\pi/\lambda$) and $\omega = 2\pi f$. While we can select radiation with a more or less well-defined wave vector \vec{k} by some kind of a monochromator, which is part of any neutron

experiment, there is fundamentally no way to select or to know the initial phase of the wave, φ_0 . For this reason, we will drop this quantity in further considerations.

The paradox here appears to be that such a plane wave occupies the whole space, instead of being point-like, while it exactly corresponds to the assumption of a well-defined, unique velocity of a classical particle. The resolution of this apparent contradiction is quite fundamental for the understanding of the scattering processes on actual samples. Except for perfect crystals (the only practical examples of which are semiconductor crystals such as Si grown for use in electronic chips), real samples have a limited coherence range, that is, the range of exactly ordered arrangement of atoms. Thus, when the neutron wave interacts with the sample, its wave properties are tested only over the extent of the coherence volume in the sample. For ordinary practical materials, including usual (nonperfect) single crystals, this volume gets as large as crystalline grains can be, that is, usually a small fraction of a millimeter. Thus, ordinary samples in actual fact are a collection of a large number of small, independent samples. Here the scattered particle will act as “point-like” with the precision of the point as defined by the coherence volume in the sample. If this volume is much smaller than the beam dimensions, we have the paradoxical classical particle propagation together with scattering on the sample as extended plane wave according to eq. (I.1.4). If the “points” defined by the coherence volumes of the sample are comparable to the beam dimensions—which never happens in soft matter samples—the classical point-like particle propagation becomes an unsatisfactory approximation.

Thus, we can conclude that (with the exception of the exotic case of large perfect single crystal samples) neutron radiation plays out the famous quantum mechanical duality in a very convenient and practical manner for us: Neutrons can be considered as perfect, exactly point-like classical mechanical particles when they travel through usual neutron scattering instruments and as infinitely extended perfect plane waves when they meet atoms inside materials. This is a very convenient picture, which simplifies the understanding of neutron scattering to a great deal.

I.1.3 NEUTRON SPIN AND OTHER PROPERTIES

Beyond its mass of 1.675×10^{-27} g, the only significant feature of a neutron particle for our purposes is its magnetic moment of $\mu = -1.913$ Bohr magneton related to its $s = 1/2$ quantum mechanical spin. The minus sign indicates that the neutron magnetic moment and its spin are oppositely oriented. The existence of a magnetic moment implies that the neutron feels magnetic fields \vec{B} via the Zeeman energy term $-\vec{\mu}\vec{B}$. This interaction can be quite substantial for magnetic fields in the range of several tesla, which neutrons most frequently encounter inside magnetic materials. It is important to keep in mind that the neutrons do not interact directly with the magnetic moments of atoms; they only see the magnetic field created by the atoms or by any other source, such as current carrying conductors.

The electric charge and electric dipole moment of the neutron are zero for all practical purposes (i.e., ongoing efforts to find them remained without success by

now), which confer the neutrons the unique property for a radiation with low energy that they can traverse large chunks of most materials, in some cases up to several meters. This also implies that the neutron radiation is very largely destruction free and biological and other soft matter samples suffer no significant radiation damage even under long irradiation in neutron scattering experiments at the most intense neutron sources.

The only mechanism for the neutron itself to damage materials is knocking out atoms from their bound position in materials. This requires that the neutrons possess sufficient kinetic energy, typically in the range of several eV, which is much more than the energy of the neutrons ideally suited for soft matter research. Nevertheless, this process, the so-called Compton scattering of neutrons, is of some interest for the investigation for fluids of light elements, such as H₂ or He. This will not be further discussed here. For the neutron energies with which we are concerned, the neutron collision with atoms inside soft matter does not break the bonds of the atoms with their neighbors, so from the point of view of mechanics the collision is actually between the neutron and the whole sample. Thus, the process is recoil free for the bound atom, with momentum change in the collision being taken up by the quasi-infinitely large mass of the sample compared to that of the neutron.

Inside matter, neutrons interact only with the nuclei of the atoms, beyond, of course, the gravity and the magnetic field. Important here is that they do not interact (for any practical purpose) with the electrons and the large electric fields inside atoms. For this reason, the neutron itself does not ionize. However, one form of the interaction with the nuclei is the absorption capture of the neutron by a nucleus, by which a new isotope is formed. If this isotope is stable, no further damage to the sample occurs. In most cases, the isotope is a short-lived “intermediate nucleus” and leads to immediate decay with emission of ionizing particles (such as α , β , or γ radiation) or the sample becomes radioactive with the decay process taking place over an extended period, which can range from hours to years. The two practical consequences of neutron absorption by certain nuclei for neutron scattering work are that (a) the high neutron absorption of a few elements (actually usually some isotopes of the element) can be a difficulty for the study of samples containing such elements and (b) samples can become radioactive in neutron scattering experiments and need to be treated with caution. On the other hand, the radiation damage to the sample by the secondary radiation after neutron absorption capture is still negligible in virtually all cases and presents no concern for the study of soft matter, in contrast to some other kinds of radiations.

I.1.4 NEUTRON INTERACTION WITH MATTER

The other form of interaction between neutrons and atomic nuclei is scattering, which in the exact terminology of nuclear physics is called “elastic scattering,” as opposed to the nuclear reactions (including absorption) between neutrons and nuclei, which are called “inelastic” in nuclear physics. We stress here, in order to avoid confusion,

8 Basic Concepts

that the notions of “elastic” and “inelastic” scattering are very different in our field of interest, the study of condensed matter by slow neutron scattering, which entirely falls into the domain of elastic processes (i.e., with no change to the particles themselves) in nuclear physics. This scattering process can be classically envisaged as the rebound of a billiard ball on another, while we must stress from the outset that this process inside condensed matter must be considered in terms of the wave properties of the particles. This is clear from our above introductory analysis, since atoms in a matter will form an ensemble of “obstacles” on the way of the neutron propagation showing a structure on a scale comparable to the neutron wavelength, that is, leading to neutron path differences between possible neutron trajectories comparable to its wavelength.

The radius of nuclei is many orders of magnitude smaller than the nm scale of atomic distances and the neutron wavelengths we are concerned with, so the nuclei can be considered as structureless points, described in space by delta functions $\delta(\vec{r}-\vec{r}_i(t))$, where $\vec{r}_i(t)$ is the position of the nucleus of atom i at time t . If we consider an atom at rest ($r_i = 0$), its interaction with the neutron wave will be described by the Fermi pseudopotential

$$V(\vec{r}) = \frac{2\pi\hbar^2}{m} b_i \delta(\vec{r}), \quad (\text{I.1.5})$$

where b_i is the so-called neutron scattering length, which characterizes the neutron interaction with the given atomic nucleus i , and its value can be found in the tables for all common isotopes of the elements (<http://www.ncnr.nist.gov/resources/n-lengths/>). Here we have to stress that the potential equation, eq. (I.1.5), is assumed to be rigid in the sense that the object that brings it about is bound to position $r = 0$ and will not recoil when hit by the neutron. As discussed above, this is exactly the situation we are concerned with here for atoms embedded in condensed matter and for this reason the relevant scattering lengths one can find in the tables are specified as “bound scattering lengths.”

It is important to observe that the scattering length b not only varies from one isotope of one element to the other (in contrast to X-rays), but can also depend on the nuclear spin:

$$b_i = b_i [1 + c_i (\vec{\sigma} \vec{I}_i)], \quad (\text{I.1.6})$$

where $\vec{\sigma}$ and \vec{I}_i are the neutron and nuclear spins, respectively, and c_i is a constant. For practical reasons that will become clear later, the scattering lengths of elements and isotopes are specified in the tables by their mean value and root mean square deviation over all isotopes in natural elements and/or over the different relative orientations of the neutron and nuclear spins. The first one

$$\bar{b}_i = \langle b_i \rangle \quad (\text{I.1.7})$$

is referred to as “coherent scattering length” and the second one

$$b_i^{\text{inc}} = \sqrt{\langle b_i^2 \rangle - \bar{b}_i^2} \quad (\text{I.1.8})$$

is referred to as “incoherent scattering length.”

It is particularly relevant for soft matter research that both the coherent and the incoherent scattering lengths of the two isotopes of hydrogen, ^1H and ^2H (or D), are substantial compared to the other elements and quite different from each other (-3.74 fm versus 6.67 fm for the coherent one and 25.27 fm versus 4.04 fm for the incoherent one). Thus, on the one hand and contrary to X-rays, with neutron scattering hydrogen atoms are well observable even if the sample contains heavier elements, and on the other hand, the substitution of a proton in a chemically well-defined position by deuteron allows us to mark and single out particular hydrogen atoms in an ensemble of many.

As pointed out above, in view of the nanoscale structure presented by atomic arrangements, the propagation of neutron radiation inside matter needs to be analyzed in terms of wave mechanics. For the point-like potential equation, eq. (I.1.5), represented by a single atom, the exact wave mechanical answer is that the incoming plane wave ϕ in eq. (I.1.4) will be transformed into a sum ϕ' of the original plane wave and a spherical wave emitted by the scattering center at $r = 0$ (cf. Figure I.1.2):

$$\phi' = e^{i(\vec{k}\vec{r}-\omega t)} + b \frac{e^{i(kr-\omega t)}}{r}. \quad (\text{I.1.9})$$

Compared to the infinitely extended plane wave, the spherical wave represents negligible particle density, so the incoming plane wave continues without

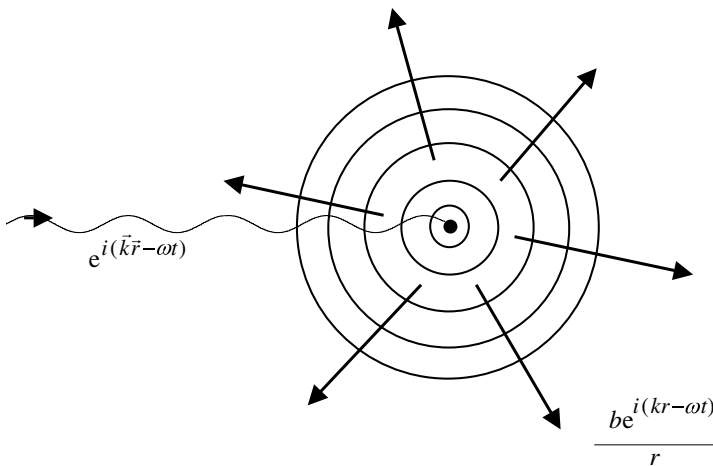


Figure I.1.2 Scattering of a neutron plane wave on a point-like fixed object generates a spherical wave with an amplitude characterized by the scattering length b .

attenuation. This is a fundamental assumption in the commonly used analysis of neutron scattering processes (the so-called first Born approximation).

This approximation is indeed perfectly sufficient for the analysis of soft matter samples, as we will see later in more detail. However, considering the propagation of the beam through a sample containing some 10^{20} atoms or more, one needs to consider the attenuation of the beam by the cumulative effects of such a large number of atoms. This can be, however (and most fortunately in view of the close to untreatable complexity it would imply otherwise), perfectly well treated in the classical point-like particle description of the neutron beam—of course again with the exception of large perfect single crystal samples, which we will simply exclude for all what follows.

I.1.5 SCATTERING CROSS SECTIONS

In order to proceed, we need to introduce the concept of scattering cross section, which tells us what a neutron detector will see in a scattering experiment, for example, in the one on a single atom as given in eq. (I.1.9). The neutron current density described by the wave function ϕ' (most commonly called “flux” and measured in units of particles/cm²/s) is given as product of the particle density and the velocity of propagation v :

$$j = |\phi'|^2 v. \quad (\text{I.1.10})$$

The detector can only be placed at a large distance from the scattering center compared to atomic dimensions, and at a position where the incoming original wave is masked out by diaphragms defining the beam. Therefore, we only need to consider at the detector the spherical wave component in eq. (I.1.9) and we will arrive at a neutron counting rate for a perfectly efficient detector of effective area F :

$$J = F \frac{b^2}{r^2} v = b^2 v \, d\Omega, \quad (\text{I.1.11})$$

where $d\Omega = F/r^2$ is the solid angle covered by the detector as looked upon from the sample at $r=0$. We realize that the incoming beam flux for the wave in eq. (I.1.4) is just identical to the velocity v , and that J is independent of the direction where the detector is placed. This allows us to introduce two commonly used cross sections, which express the scattered particle current onto a detector surface by the area over which the same number of particles arrive by unit time to the sample:

$$\frac{d\sigma}{d\Omega} = b^2 \quad \text{and} \quad \sigma = 4\pi b^2. \quad (\text{I.1.12})$$

The first of these is the “differential cross section” and the second the “total cross section.” The first one characterizes the measurable scattered beam intensity around a given detector position and the second one the scattered beam intensity integrated

over all directions. Of course, these expressions give the cross sections only for a single bound atom, described by the potential equation, eq. (I.1.4). The cross sections for an ensemble of atoms will be considered below, and we will see that it delivers a lot of information on the atomic structure and atomic motion in the ensemble.

The total cross sections σ , as defined by eq. (I.1.12), are also given in the usual tables (<http://www.ncnr.nist.gov/resources/n-lengths/>) in units of barn = 10^{-24} cm², for both coherent and incoherent scattering lengths. In view of eq. (I.1.8), the sum of coherent and incoherent scattering cross sections gives the grand total per atom in average over all nuclear spin states and all isotopes in the natural element. It is worth recalling that the typical diameter of an atom is in the range of Å, so the geometrical cross section presented by the atom to the neutron beam is in the 10^{-16} cm² range, while neutron scattering cross sections are less than 100 barn = 10^{-22} cm². This illustrates the good validity of eq. (I.1.9): only a most tiny fraction of the incoming beam hitting an atom is scattered. The cross section, on the other hand, is quite comparable to the geometrical cross section of the nuclei themselves.

The cross section is also a practical way to describe the probability of absorption of neutron by atoms, with the help of the so-called absorption cross section σ^{abs} , defined analogously to the one introduced in the text before eq. (I.1.12). It is a good illustration of the intensity of the strong interaction (which acts between neutrons and nuclei, in form of both scattering and absorption) that σ^{abs} can be much larger than the geometrical cross section of the nucleus. The absorption of neutrons happens independently, without correlation between atoms; the process can be evaluated by adding up the cross sections for the atoms in a sample. For example, if a sample contains n_i atoms/cm³ with an average cross section $\bar{\sigma}_i^{\text{abs}}$, the attenuation of the neutron beam will be given as

$$J(x) = J_0 \exp(-xn_i\bar{\sigma}_i^{\text{abs}}), \quad (\text{I.1.13})$$

where x is the distance in the direction of the neutron beam propagation and $1/n_i\bar{\sigma}_i^{\text{abs}}$ is the penetration range of neutrons for the material.

Note that in the general quantum mechanical formalism the scattering length b is treated as a complex number and the absorption cross section is then related to its imaginary part. This imaginary part will also result in eq. (I.1.9) in a small shift of the phase of the spherical wave. However, the imaginary part of b is in practice only large enough to become measurable for a couple of very highly absorbing isotopes, and for most materials the cross-section tables only cite the real part of b and the absorption cross section itself. Thus, in what follows we implicitly assume that the neutron scattering length b is a real number for all the atoms we have to do with in soft matter. Nevertheless, in order to keep some formulas in the usual more general form, whenever it does not make matter more complicated, we will formally keep the distinction between b and its complex conjugate b^* (and also for related quantities).

The absorption cross section for most isotopes is inversely proportional to the neutron velocity for the slow neutrons we are interested in (as it depends on the period of time the neutron spends near the absorbing nucleus), with the notable exception of a few very highly absorbing isotopes, such as ¹⁵⁷Gd.

12 Basic Concepts

There is a final notion related to cross sections we need to introduce: that of elastic and inelastic scattering processes. Eq. (I.1.9) describes an elastic scattering process, since the wave number (momentum) of the outgoing scattered radiation, which becomes in good approximation a plane wave with wave number k at macroscopic distances from the sample, is the same as the wave number of the incoming beam. Thus, incoming and outgoing neutrons have the same velocity, that is, energy. This would not be the case, for example, if we would consider scattering on an object moving with respect to the neutron beam direction. In this case, Doppler effect will occur; for example, if the scattering object moves opposite to the neutron beam with velocity v_0 , the rebounding neutron will have higher velocity than the incoming one, and this velocity change will reach a maximum $2v_0$ in the direction of backward scattering. This can be easily demonstrated by considering a reference frame in which the scattering object is at rest. Atoms do move in soft matter objects, either around a quasi-equilibrium position or in a diffusive manner or in more complex ways. So the scattered neutron energy $E' = \hbar^2 k'^2 / 2m$ can be different from the incoming neutron energy E . Analogously to the differential cross section, this process can be characterized by the so-called “double differential cross section”

$$\frac{d^2\sigma}{dE' d\Omega}, \quad (\text{I.1.14})$$

which accounts for the neutrons that reach the detector of solid angle $d\Omega$ with an outgoing final neutron energy within a given energy interval with width dE' .

Note that the scattering cross section in the tables (<http://www.ncnr.nist.gov/resources/n-lengths/>) usually refers to a single atom. In practice, cross sections are more often evaluated for one chemical formula unit of the sample, instead of one atom.

I.1.6 BEAM PROPAGATION THROUGH SAMPLES

Let us now consider in more detail what happens if instead of just one atom, neutrons scatter on ensemble of bound atoms, each of them described by a Fermi pseudo-potential function similar to eq. (I.1.5). For our purpose, we will be mostly concerned with the superposition of the scattered spherical waves, which will produce a complex pattern of interference between the waves scattered from the individual atomic nuclei, following the many centuries old Huygens principle. Before turning our focus to this final point, we will complete the discussion of the first term in eq. (I.1.9), that is, the fate of the nonscattered part of the incoming beam.

On the one hand, the neutron beam will get attenuated by the absorption when going through substantial amount of matter, as discussed above, and also by the scattering, even if this attenuation could be perfectly neglected when considering only one atom, as in eq. (I.1.9). Although, in contrast to absorption, the total scattering cross section of materials is not simply the sum of the scattering cross sections of the atoms it contains (as we will see in detail below), this is a good rough approximation, in particular for noncrystalline matter and for neutrons with

wavelength not greater than about 5 \AA . This implies to replace in eq. (I.1.13) the average absorption cross section by the sum of the average absorption and scattering cross sections $\bar{\sigma}_i^{\text{abs}} + \bar{\sigma}_i^{\text{scatt}}$ (cf. <http://www.ncnr.nist.gov/resources/n-lengths/>).

The attenuation range $\Lambda = 1/n_i(\bar{\sigma}_i^{\text{abs}} + \bar{\sigma}_i^{\text{scatt}})$ is a characteristic parameter for different materials, and it can range from a few μm for highly absorbing materials to a substantial fraction of a meter. Due to the high incoherent cross section of the proton (80.3 barn), organic materials containing high density of hydrogen show strong attenuation ($\Lambda \sim 0.1\text{--}0.2 \text{ mm}$), while heavy materials, such as steel, can be quite transparent for neutrons with $\Lambda \sim 1\text{--}10 \text{ cm}$, depending on the specific composition of the alloy; for example, Fe displays low absorption, while Co absorbs more than 10 times stronger than Fe. For X-rays, the contrast is quite the opposite: organic matter is generally quite transparent compared to highly absorbing metals.

The attenuation of the neutron beams in matter is being used in neutron radiography, where essentially the neutron shadow of objects is recorded with high-resolution position-sensitive neutron imaging detectors (usually optically recorded scintillator plates), which can achieve above $20 \mu\text{m}$ resolution. This method is widely used to detect holes, cracks, or highly absorbing organic materials inside metallic parts. The most widespread application is the routine check of airplane jet engine turbine blades for the presence of oil coolant in the cavities inside the blades.

Neutron tomography came of age more recently. It consists of taking the radiographic image of an object in different directions and creating—using well-established computer tomography algorithms—a three-dimensional picture of the object, which can reveal internal structures not accessible to other observation tools without destroying the sample. This method is particularly precious in engineering and in the study of valuable archeological artifacts, as also shown in Figure I.1.3 (Kardjilov et al., 2006).

I.1.7 REFRACTION AND REFLECTION

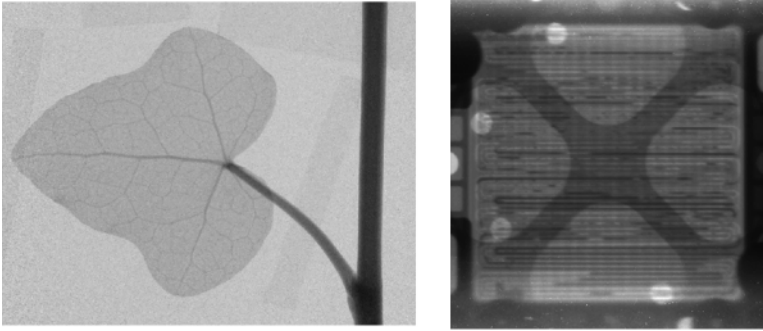
On the other hand, the volume average of the potential equation, eq. (I.1.4), of all atomic nuclei will represent a small, but not always negligible contribution to the potential energy felt by the nonscattered part of the wave in eq. (I.1.9) or for the same matter, the classical particle it corresponds to. This potential will depend on the so-called “scattering length density” of the sample ρ_{scatt} , which is the product of the atomic density ρ_a and the average scattering length over all atoms in the sample \bar{b} . In inhomogeneous, layered, and other nanostructured materials, ρ_{scatt} can be a function of the position \vec{r} . Thus, we have a total locally averaged potential relevant for the propagation of the nonscattered beam:

$$U(\vec{r}) = mgh - \mu B(\vec{r}) + \frac{2\pi\hbar^2}{m} \rho_{\text{scatt}}(\vec{r}). \quad (\text{I.1.15})$$

Here the first term is the gravitational energy, which turns the neutron trajectories into free fall parabolas, in some cases significantly different from straight lines. The other two terms have been discussed in detail above. Note that in ferromagnetic materials

14 Basic Concepts

(a)



(b)

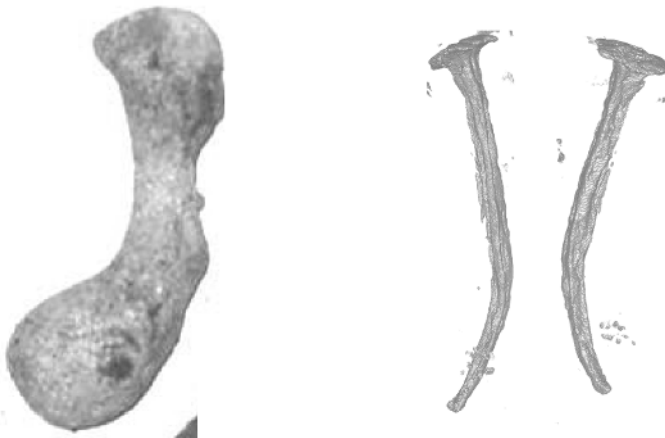


Figure I.1.3 Examples of neutron imaging. (a) Neutron radiography (shadow image) of a plant leaf (left) and a fuel cell (right). In the latter image, the dark horizontal lines show the distribution of water inside the closed cell. (b) Neutron computer tomography reconstruction in three dimensions of an object (nail in different views, right) hidden inside an archaeological calcareous concretion shell (left).

the saturation magnetization \vec{M} contributes to the local value of the magnetic field \vec{B} (averaged over interatomic atomic distances) by the substantial amount of $4\pi\vec{M}$.

For most materials, the potential in eq. (I.1.15) corresponds to a potential barrier in the range of up to some 100 neV; that is, the neutrons need to exceed a critical velocity v_c of up to about 5 m/s in order to be able to enter the sample. This is quite a small velocity in general, but it comes to prominent significance in the case the neutrons approach an optically flat surface at a small grazing angle. If the component of the neutron velocity perpendicular to the surface is inferior to v_c , the neutron will be totally reflected. This leads to a critical angle of $\theta_c = \arcsin(v_c/v)$, which can amount to about 0.5° for 5 Å wavelength neutrons.

At grazing angles ranging between θ_c and few times this value, we observe a range of significant partial reflectivity, whose investigation leads to the fast growing field of neutron reflectometry in the past three decades. This chapter of modern

neutron research is based on the fact that the reflectivity curve $R(\theta)$ for $\theta > \theta_c$ is determined by the variation of the scattering length density function in the direction z perpendicular to the optically flat sample surface, $\rho_{\text{scatt}}(z)$. For example, in a periodic multilayer system one can observe sizable peaks in the reflectivity curve $R(\theta)$, analogous to the Bragg peaks in crystalline matter. For magnetic multilayer structures, the reflectivity might depend very strongly on whether the neutron magnetic moment is oriented parallel or antiparallel to the magnetic field B applied in order to align the magnetization in the layers, cf. eq. (I.1.15). This way magnetic multilayers can serve as powerful neutron beam polarizers by reflecting neutrons with one spin direction with much higher probability than those with the other (Mezei and Dagleish, 1977). A detailed description of the art of neutron reflectometry can be found in Chapter II.2.

I.1.8 SCATTERING, INTERFERENCE, AND COHERENCE

We now turn our attention to the evaluation of the interference processes that can occur between neutron waves scattered by different atoms. This is the central subject for the study of matter on the atomic scale by actually any radiation (even including electron microscopy, where the atomic scale resolution often apparently achieved by direct imaging is also the result of shrewd processing and reconstruction). When particle waves scattered on different atoms are superposed, the interference between these waves is determined by the optical path length differences between waves scattered at different atoms. The optical path is defined as the real geometrical distance in the direction of wave propagation multiplied by the wave number of the radiation, cf. $\vec{k}\vec{r}$ in eq. (I.1.4). A change of the optical path comparable to unity implies substantial modification of the wave by a shift of its phase by a radian. Hence, the high sensitivity of neutron wave interference to distances comparable to $1/k = \lambda/2\pi$ offers us a spatial resolution capability not accessible by direct imaging methods.

Let us consider the optical paths for scattering on a point-like object (nucleus) at a position \vec{r}_i , by comparing it to the optical path for a scattering object at $r = 0$. The incoming radiation will be considered as a plane wave with wave vector \vec{k} and the outgoing radiation as spherical waves from each scattering center with a wave number k' , cf. eq. (I.1.9). Here we assume that the detection point is at a very large distance compared to the distance between the scattering points; therefore, the outgoing radiation arrives to the detector practically as a plane wave with wave vector \vec{k}' , with a direction determined by the position of the neutron detection. As shown in Figure I.1.4, the optical path difference between the two spherical waves scattered at the origin and \vec{r}_i will be given by

$$\delta s = |\vec{k}\vec{r}_i| + |\vec{k}'\vec{r}_i| = -\vec{q}\vec{r}_i, \quad (\text{I.1.16})$$

where $\vec{q} = \vec{k}' - \vec{k}$ is the so-called momentum transfer vector. If we have to do with elastic scattering, that is, the absolute value of \vec{k}' is equal to that of \vec{k} (i.e., k), then we

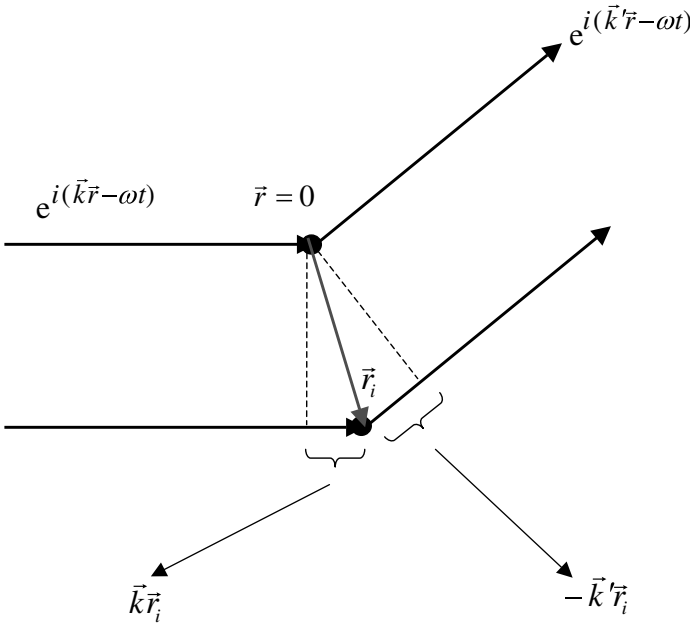


Figure I.1.4 Optical path difference for scattering on a point-like object at position \vec{r}_i compared to scattering at $r=0$.

will find that $q = 2k \sin(\theta/2)$, where θ is the angle between the incoming and outgoing radiations, the so-called scattering angle.

Thus, analogously to eq. (I.1.9), the scattered beam wave function becomes (omitting in what follows the nonscattered part of the incoming beam)

$$\phi' = b \frac{e^{i(k'r - \omega't)}}{r} + b_i \frac{e^{i(k'|\vec{r} - \vec{r}_i| - \omega't)}}{|\vec{r} - \vec{r}_i|} \cong \frac{e^{i(k'r - \omega't)}}{r} (b + b_i e^{-i\vec{q}\vec{r}_i}), \quad (\text{I.1.17})$$

where we took into account that the detector is at a distance r very much larger than the distance between the scattering nuclei r_i . Note that eq. (I.1.9) is valid for a fixed, rigid scattering center and implies elastic scattering with equal absolute values $k = k'$, so this will also apply for the ensembles of scattering objects considered in the next paragraphs. The square of absolute value of the wave function (i.e., the finding probability) thus becomes

$$|\phi'|^2 \cong \frac{1}{r^2} |(b + b_i e^{-i\vec{q}\vec{r}_i})|^2 = \frac{1}{r^2} |b + b_i \cos(\vec{q}\vec{r}_i) - ib_i \sin(\vec{q}\vec{r}_i)|^2 \quad (\text{I.1.18})$$

and following the definition of cross section in eqs. (I.1.10)–(I.1.12) we arrive at the scattering cross section

$$\frac{d\sigma}{d\Omega} = [b^2 + 2bb_i \cos(\vec{q}\vec{r}_i) + b_i^2]. \quad (\text{I.1.19})$$

Eq. (I.1.19) illustrates how we can observe atomic scale structures by observing the neutron scattering cross section as a function of the momentum transfer vector \vec{q} . From its definition in connection with eq. (I.1.16), we can see that the simplest way to vary \vec{q} is to observe the scattering at different scattering angles and we can also change the direction of \vec{r}_i by rotating the sample. Thus, in this simplest example given in eq. (I.1.19), one will be able to determine both the distance between the two atoms with a good precision on the Å length scale and their scattering lengths b and b_i , which could help to identify them. As a matter of fact, diatomic molecules in a low-density gas are a practical example for this trivial model, if the motion of these molecules is slow enough that it can be neglected.

Two fundamental assumptions have been implicitly used in deriving eqs. (I.1.16)–(I.1.19): (a) the incoming radiation for both scattering objects is the same plane wave with wave vector \vec{k} and (b) the outgoing radiation for both scattering objects has the same wave vector \vec{k}' (which also implies the same frequency). Point (b) is a simple practical requirement: the optical path length difference between radiations with different wave vectors would depend on the exact position of the neutron detection. Since neutron detection happens randomly within a macroscopic volume in the detectors, such a dependence of neutron paths leads to an averaging over a broad distribution of relative phase differences of the superposed waves; thus, no interference effect will be observable.

Point (a) is a more fundamental restriction: there is no way to prepare an incoming neutron beam in which wave components with different wave vectors \vec{k} would display a correlation of the initial phases φ_0 (“random phase theorem”). Although one can mathematically easily write down wave functions with such phase correlation (coherence) between different components with different wave numbers (as it is done in textbooks discussing quantum mechanical “wave packets” of different “coherence lengths”), with real-life elementary particles such as neutrons there is no method known to reproduce such a wave packet with identical relative phases between components with different wave numbers. This is one of the most fundamental points in understanding the radiation created by some kind of thermodynamic processes (as opposed to macroscopically generated radiation, like a resonating cavity driven by a radio frequency power supply): every wave is only coherent with “itself”; that is, there is no coherence between radiations with different wave vectors \vec{k} . Therefore, all considerations in neutron scattering make physical sense only if they refer to a perfectly well-defined neutron wave vector (and hence neutron velocity), and all radiation must be considered as an incoherent, classical ensemble of particles with infinitely well-defined velocities/wave vectors. In view of our introductory discussion, coherence between different neutron wave components can practically only be generated by the scattering process in the sample, for example, in eq. (I.1.9) between the plane and spherical wave components.

I.1.9 CROSS SECTIONS AND PAIR CORRELATION FUNCTIONS

Eq. (I.1.18) can be readily generalized to derive the general expression of the cross section for elastic scattering on an arbitrary ensemble of atoms. Let us describe

the ensemble of atoms by a microscopic scattering length density function $\rho(\vec{r})$, in which each nucleus will appear as a delta function in view of eq. (I.1.5). Thus, in contrast to the average scattering length density function ρ_{scatt} introduced above, the microscopic scattering length density function reflects the atomic structure in all details. Then the sum over the two scattering objects in eq. (I.1.18) needs to be extended to an integral over the whole volume of the sample, and similarly to eq. (I.1.17) we get for the scattering cross section

$$\begin{aligned} \frac{d\sigma}{d\Omega} &= \left| \int_V \rho(\vec{R}) e^{-i\vec{q}\vec{R}} d\vec{R} \right|^2 = \int_V \rho^*(\vec{R}) e^{i\vec{q}\vec{R}} d\vec{R} \int_V \rho(\vec{R}) e^{-i\vec{q}\vec{R}} d\vec{R} \\ &= \int_V \int_V \rho^*(\vec{R}) \rho(\vec{R}') e^{i\vec{q}\vec{R} - i\vec{q}\vec{R}'} d\vec{R} d\vec{R}', \end{aligned} \quad (\text{I.1.20})$$

where the integrations are made over the volume of the sample, V . We introduce as new variable the distance between points \vec{R} and \vec{R}' , that is, $\vec{r} = \vec{R}' - \vec{R}$:

$$\frac{d\sigma}{d\Omega} = \iint_V \rho^*(\vec{R}) \rho(\vec{R} + \vec{r}) e^{-i\vec{q}\vec{r}} d\vec{R} d\vec{r} = \int_V d\vec{R} \int_V \rho^*(\vec{R}) \rho(\vec{R} + \vec{r}) e^{-i\vec{q}\vec{r}} d\vec{r}. \quad (\text{I.1.21})$$

Here the first integration is a summation over the volume of the sample, which effectively means an averaging of the second integration over the whole volume of the sample:

$$\frac{d\sigma}{d\Omega} = \int_V \langle \rho^*(\vec{R}) \rho(\vec{R} + \vec{r}) \rangle e^{-i\vec{q}\vec{r}} d\vec{r} = \int_V g(\vec{r}) e^{-i\vec{q}\vec{r}} d\vec{r} = S(\vec{q}). \quad (\text{I.1.22})$$

As mentioned above, the cross section is usually expressed per some essentially freely defined unit amount of the sample matter, usually chemical formula unit, characteristic atoms, and elementary structural unit, among others. This normalization is included here in the definition of the averaging under the $\langle \cdot \cdot \rangle$ sign. To calculate the total scattering power of the amount of material in the actual sample, one needs to determine the number of reference units contained in the sample volume. Fundamentally, the total cross section of the sample should be proportional to its total volume, which is indeed the case if the beam does not suffer essential attenuation within the sample. To correct for such “self-shielding” effect, we have to consider the beam attenuation factors discussed above.

The average indicated by $\langle \rho^*(\vec{R}) \rho(\vec{R} + \vec{r}) \rangle = g(\vec{r})$ is called the pair correlation function and gives the probability of finding a particle in the sample at position $\vec{R} + \vec{r}$ if there is one at position \vec{R} . So this function describes the correlations between atoms in the sample. In noncrystalline materials, all directions are equivalent; thus, $g(r)$ becomes a function of the absolute value of the distance r . If, for example, there are

no atoms (i.e., atomic nuclei) in the sample at distance r from each other, $g(r)$ will be zero. This is the case for distances shorter than the minimum separation of nearest neighbors. In contrast, in amorphous matter $g(r)$ has a maximum at around the average distance of nearest neighbors.

The integrals in eq. (I.1.22) are, paradoxically, independent of the sample volume. In particular in noncrystalline matter, but also in polycrystalline samples or nonperfect single crystals, there is a characteristic correlation length ξ in the sample structure: there will be no correlation between the positions of atoms further apart than this distance. It is easiest to envisage this in a polycrystalline material. There is a periodic order between atoms within one crystalline grain, but beyond that the relative positions are random. This is expressed by behavior of $g(r)$ for $r > \xi$. It will tend to a constant, the square of the mean scattering density $\bar{\rho}^2$, and the integration of the periodic function e^{-iqr} will average to zero for $r > \xi$. Thus, the so-called “structure factor” $S(\vec{q})$, defined in eq. (I.1.22) as the Fourier transform of the correlation function $g(\vec{r})$, will have a value independent of the integration volume considered, if it extends over the range of correlation ξ .

This observation contains one of the other fundamental facts about neutron scattering and similar experiments. A macroscopic sample in fact consists of a multitude of independent samples with the dimension of the sample correlation length ξ and what we measure is the average behavior of these myriads of subsamples within the typically cm^3 large sample volume. The real physical sample volume, the coherence volume of the order of ξ^3 in soft matter or polycrystalline samples, typically ranges from 10^{-22} to some 10^{-6} cm^3 . So indeed, the observed cross sections are good averages over the many possible atomic configurations and orientations to realize the more or less short-range local atomic order characterizing the material we are concerned with.

We will come back to the exact interpretation of the cross section formulas, eqs. (I.1.20)–(I.1.22), we were able to deduce in rather conspicuous matter: simple mindedly, adding the spherical waves emitted by all atoms in the sample, à la Huygens. This simple approach shows clearly the mechanism involved, how the interference between these individual spherical waves carry information on the atomic arrangement, cf. the example of eqs. (I.1.16)–(I.1.19). Nevertheless, there is an important underlying approximation: the atoms are not rigid in a real sample; there is always some degree of motion. The exact theory, which indeed contains no approximation with the one exception that the sample has to be small enough to avoid substantial beam attenuation, is due to van Hove (1954). It is mathematically more complex and less evident to visualize. Its result is, however, just a very plausible generalization of eq. (I.1.22).

I.1.10 DYNAMIC STRUCTURE FACTOR

Let us define a more general pair correlation function similar to $g(\vec{r})$ in eq. (I.1.22):

$$g(\vec{r}, t) = \langle \rho^*(\vec{R}, 0) \rho(\vec{R} + \vec{r}, t) \rangle. \quad (\text{I.1.23})$$

This van Hove correlation function expresses the probability that, if there was an atom at position \vec{R} at time 0, we will find an atom at a location displaced by \vec{r} at a later time t . Then the double differential cross section will be determined by the space–time Fourier transform of correlation function, eq. (I.1.23):

$$\frac{d^2\sigma}{d\Omega dE'} = \frac{k'}{k} \int_V d\vec{r} \frac{1}{2\pi\hbar} \int_{-\infty}^{\infty} g(\vec{r}, t) e^{-i(\vec{q}\vec{r}-\omega t)} dt = \frac{k'}{k} S(\vec{q}, \omega). \quad (\text{I.1.24})$$

$S(\vec{q}, \omega)$ is the so-called “scattering function” or “dynamic structure factor” and the origin of the prefactor k'/k is the fact that the neutron current density is proportional to the beam velocity, cf. eq. (I.1.10). One important feature of this exact result is that the scattering function as defined in the expression of the double differential cross section in eq. (I.1.24) is a function of two parameters describing the scattering process only: the momentum transfer \vec{q} , as introduced in eq. (I.1.16), and the neutron energy transfer $\hbar\omega = E' - E$, where E and E' are the incoming and outgoing neutron energies $mv^2/2$, respectively. The often considered intermediate scattering function is

$$I(\vec{q}, t) = \int_{-\infty}^{\infty} S(\vec{q}, \omega) e^{-i\omega t} d\hbar\omega \equiv \int_V g(\vec{r}, t) e^{-i\vec{q}\vec{r}} d\vec{r}. \quad (\text{I.1.25})$$

It is of particular practical significance in model calculations and in neutron spin echo (NSE) spectroscopy (cf. later in this book).

With the exact results, eqs. (I.1.24) and (I.1.25), at hand, we can now return to the interpretation of the time-independent correlation function $g(\vec{r})$ involved in “elastic” scattering experiments, cf. eq. (I.1.22). If it is defined to describe the correlations at a given moment of time, say $t = 0$ (“equal time” or “static” correlation function), then it will correspond to the intermediate correlation function at $t = 0$, that is,

$$I(\vec{q}, t = 0) = \int_{-\infty}^{\infty} S(\vec{q}, \omega) d\hbar\omega = \int_{-\infty}^{\infty} \frac{k}{k'} \frac{d^2\sigma}{d\Omega dE'} dE' = S(\vec{q}) = \int_V g_{\text{stat}}(\vec{r}) e^{-i\vec{q}\vec{r}} d\vec{r}. \quad (\text{I.1.26})$$

The integration of the double differential cross section here over all energy changes is feasible only within a more or less fair approximation. In the so-called “elastic” neutron scattering experiments, in which the final neutron energy is not analyzed, only the angular dependence of the scattered neutron intensity is determined (e.g., diffraction). The expression “elastic” is fully misleading here, actually what one tries to accomplish is just to integrate over all energy transfers in order to obtain the differential cross section $d\sigma/d\Omega$. The rough approximation here is that for neutron energy changes corresponding to the frequencies of atomic motion in soft matter the wave number of the scattered neutrons k' will span a substantial range and a given

scattering angle will not correspond to scattering with a given momentum transfer q , cf. the comments after eq. (I.1.16). The kinematic prefactor k/k' is also not taken care of in such an “elastic” experiment. The smaller the deviations from an apparent q (Placek corrections), the higher the incoming neutron energy. As a matter of fact, with the very high energies of X-rays in the 10 keV range, these deviations become negligible and the static X-ray structure factor $S_X(\vec{q})$ can indeed be directly observed in view of the inherently correct integration over the energy in “elastic” X-ray experiments, cf. eq. (I.1.26).

On the other hand, eq. (I.1.22) will exactly hold, corresponding to its derivation for a rigid array of atoms, if we define the correlation function g as the one for infinite times $g_{\text{avr}}(\vec{r})$, that is, looking at the correlations in the long time average of the scattering density $\rho_\infty(\vec{r})$. This will correspond to the real elastic scattering with energy change $E = 0$, which of course can only be exactly determined experimentally by using an energy discrimination method to single out the elastic scattering contribution. This can be equated to the $t = \infty$ limit of the intermediate scattering function. However, in solid samples and in particular at low temperatures, much of the scattering is elastic (e.g., Bragg peaks in crystalline matter), so the “elastic” scattering experimentation (i.e., without analyzing the scattered beam energy) indeed corresponds to mostly elastic scattering, and there is little difference between the static ($t = 0$ “equal time”) correlations and the “time-averaged” ($t = \infty$) correlations.

I.1.11 DEBYE–WALLER FACTOR: COHERENT AND INCOHERENT SCATTERING

It is also worth evaluating eq. (I.1.20) for the case when the neutron scattering density $\rho(\vec{r})$ corresponds just to the sum of δ functions corresponding to different nuclei i with scattering lengths b_i at locations \vec{r}_i , that is, $\sum b_i \delta(\vec{r} - \vec{r}_i(t))$. We readily get

$$\frac{d\sigma}{d\Omega} = \left| \sum_i b_i e^{-i\vec{q}\vec{r}_i} \right|^2 = \sum_{i,j} b_i^* b_j e^{i\vec{q}(\vec{r}_j - \vec{r}_i)}. \quad (\text{I.1.27})$$

This case applies only to the static $t = 0$ equal time correlations, since only at a well-defined time instant can the atomic nuclei be assigned to δ functions at exact positions.

In contrast, the long time average even for nuclei stationarily sitting at equilibrium positions will be, instead of a δ function, a density distribution function with a width corresponding to the amplitude of the vibrational atomic motions around the equilibrium positions. In the simplest approximation, these displacements in time will lead to a Gaussian distribution of the time-averaged probability of finding an atom around its equilibrium position, for example,

$$\rho_{i,\infty}(\vec{u}) \propto e^{-x^2/2\sigma_{i,x}^2 + y^2/2\sigma_{i,y}^2 + z^2/2\sigma_{i,z}^2}, \quad (\text{I.1.28})$$

where x , y , and z are the coordinates of the displacement $\vec{u} = \vec{R} - \vec{r}_i$ and $\sigma_{i,x}$ is the root mean square displacement of atom i from the equilibrium position \vec{r}_i in the x -direction. This then leads to the time-averaged density function for the whole sample:

$$\rho_\infty(\vec{R}) = \sum_i b_i \rho_{i,\infty}(\vec{R} - \vec{r}_i) \quad (\text{I.1.29})$$

and the integration by \vec{R} in eq. (I.1.20) will result in Fourier transforming $\rho_{i,\infty}(\vec{r})$ into the so-called structure factor $f_i(\vec{q})$ (or thermal factor), and eq. (I.1.27) becomes for the exactly elastic scattering representing the time-averaged structure

$$\left(\frac{d\sigma}{d\Omega} \right)_{\text{elastic}} = \left| \sum_i b_i f_i(\vec{q}) e^{-i\vec{q}\vec{r}_i} \right|^2 = \sum_{i,j} b_i^* b_j f_i^*(\vec{q}) f_j(\vec{q}) e^{i\vec{q}(r_j - r_i)}. \quad (\text{I.1.30})$$

In a system that is symmetric to the change of the direction of the coordinates (e.g., x to $-x$), the structure factors f_i have real values. Also note that $f_i(0) = 1$ by definition, which is the consequence of the conditions that $\int \rho_{i,\infty}(\vec{r}) d\vec{r} = b_i$, since $\rho_{i,\infty}(\vec{r})$ describes how the time average of the finding probability of the one atom i is distributed in space.

Let us assume that all atoms in the sample perform isotropic thermal vibrations around their equilibrium positions by about the same amplitude, which can be characterized by the mean square displacement $\langle u^2 \rangle$ around the equilibrium positions. Then the Gaussian distribution in eq. (I.1.28) takes the form $\exp(-r^2/2\langle u^2/3 \rangle)$ and its Fourier transform becomes $f_i(\vec{q}) = \exp(-q^2\langle u^2 \rangle/6)$, that is, $f_i^*(\vec{q})f_j(\vec{q}) = \exp(-q^2\langle u^2 \rangle/3)$. Finally, eq. (I.1.30) can be written as

$$\left(\frac{d\sigma}{d\Omega} \right)_{\text{elastic}} = e^{-2W} \left| \sum_i b_i e^{-i\vec{q}\vec{r}_i} \right|^2 = e^{-2W} \sum_{i,j} b_i^* b_j e^{i\vec{q}(r_j - r_i)}. \quad (\text{I.1.31})$$

Here the so-called Debye–Waller factor $e^{-2W} = \exp(-q^2\langle u^2 \rangle/3)$ can be approximated at small mean square displacements (moderate temperatures) as $e^{-2W} = 1 - q^2\langle u^2 \rangle/3$.

Note that for magnetic atoms the structure factor plays a more fundamental role and it is only marginally related to the thermal vibrations of the atoms. As we have pointed out above, the neutrons by their magnetic moment also see the magnetic fields, cf. eq. (I.1.15). The magnetism of atoms comes from their electrons, not from the point-like nuclei, so the strong microscopic magnetic field characterizing each magnetic atom extends practically over the whole atomic diameter. For this reason, the atomic magnetic interaction for the neutron corresponds to a density distribution over the whole electron cloud of the atom (i.e., it reaches out for far larger distances than the atomic vibrations in a solid) and consequently the corresponding magnetic scattering length will need to be characterized including a structure factor $f_M(\vec{q})$ defined with a normalization such that $f_M(0) = 1$. Thus, in eq. (I.1.27) for the

magnetic atoms we have to replace b_i by $b_i + p_i^{\text{eff}} f_M(\vec{q})$, where the magnetic scattering length of the atom p_i^{eff} depends in an intricate manner on the neutron spin and atomic magnetization, including their relative orientation. These more special aspects of magnetic neutron scattering will not be discussed here; the interested reader is referred to the literature (Squires, 1978).

We will conclude this introduction to the basic features of neutron scattering by a discussion of coherent and incoherent scattering. It was pointed out above that the scattering length b_i for a given atomic species can depend on further details of the nuclei involved, for example, many elements have different isotopes and many isotopes have nuclear spin and hence different nuclear spin states. We will examine the consequence of this in mathematical detail for the simple expression of the cross section, eq. (I.1.27), and will generalize the result to the van Hove cross-section formula by analogy. Let \bar{b}_i denote the average scattering length for a given atomic species (e.g., Ni, which has many isotopes, or ^1H , which can display different spin states with respect the neutron spin), as discussed in connection with eqs. (I.1.7) and (I.1.8). We will then explicitly split the terms in the sum in eq. (I.1.27) into the average values and the deviations from the average:

$$\frac{d\sigma}{d\Omega} = \sum_{i,j} (\bar{b}_i^* \bar{b}_j + b_i^* b_j - \bar{b}_i^* \bar{b}_j) e^{i\vec{q}(r_j - r_i)} = \sum_{i,j} \bar{b}_i^* \bar{b}_j e^{i\vec{q}(r_j - r_i)} + \sum_{i,j} (b_i^* b_j - \bar{b}_i^* \bar{b}_j) e^{i\vec{q}(r_j - r_i)}. \quad (\text{I.1.32})$$

The key of the matter now is to remember that in any sample (except perfect crystals) we have a correlation length ξ beyond which the atoms are randomly placed and therefore do not contribute to the sums involved here. So in actual fact each sample has to be considered as an ensemble of a large number of independent, distinct “subsamples” of the material studied, and the cross section will be an average over all these subsamples. The first sum on the right-hand side of eq. (I.1.32) is the same for all subsamples, and it is called “coherent” scattering. Considering the average of any element (i, j) in the second sum over all subsamples, we need to keep in mind the definition of the average value $\bar{b}_j = \langle b_j \rangle$. Since under ordinary conditions isotopes and nuclear spins states are fully randomly distributed in the sample, there is no correlation between the occupations of site i and site j by these possible choices. Therefore, if $i \neq j$

$$\langle b_i^* b_j - \bar{b}_i^* \bar{b}_j \rangle = \langle b_i^* \rangle \langle b_j \rangle - \bar{b}_i^* \bar{b}_j \equiv 0 \quad (\text{I.1.33})$$

while for $i = j$

$$\langle b_i^* b_i - \bar{b}_i^* \bar{b}_i \rangle = \langle b_i^* b_i \rangle - \bar{b}_i^* \bar{b}_i = (b_i^{\text{inc}})^2 \quad (\text{I.1.34})$$

in view of the definition of the incoherent scattering length in eq. (I.1.8), which is introduced under the practical assumption that b_i are real numbers

(<http://www.ncnr.nist.gov/resources/n-lengths/>). Thus, eq. (I.1.32) becomes

$$\frac{d\sigma}{d\Omega} = \sum_{i,j} \bar{b}_i^* \bar{b}_j e^{i\vec{q}(r_j-r_i)} + \frac{1}{4\pi} \sum_i \sigma_i^{\text{inc}}. \quad (\text{I.1.35})$$

Similarly we can rewrite eq. (I.1.33):

$$\left(\frac{d\sigma}{d\Omega}\right)_{\text{elastic}} = \sum_{i,j} \bar{b}_i^* \bar{b}_j f_i^*(\vec{q}) f_j(\vec{q}) e^{i\vec{q}(r_j-r_i)} + \frac{1}{4\pi} \sum_i |f_i(\vec{q})|^2 \sigma_i^{\text{inc}}. \quad (\text{I.1.36})$$

In practical terms, in particular in soft matter or matter in other than solid phase, the elastic scattering is defined by the resolution of the spectrometer used to distinguish between elastic and inelastic scattering contributions. So the structure factors and, for the same matter, the mean square displacements of atoms depend on the timescale selected to build the averages $\bar{\rho}_i(\vec{r})$ and $\langle u_i^2 \rangle$, as determined by the experimental resolution δE of the spectrometer by the relation $t_{\text{avr}} = \hbar/\delta E$. With this definition of the averaging timescale kept in mind, the experimentally determined factor $|f_i(\vec{q})|^2$ in eq. (I.1.36) is called the incoherent elastic structure factor (EISF). It describes the Fourier transform of the probability distribution $\bar{\rho}_i(\vec{r})$ of finding atom i at different locations around its average position over the averaging time t_{avr} . For example, for a hydrogen bond with a proton tunneling back and forth between two positions, this distribution will consist of two spots (broadened by vibrations) where the atom can be.

The plausible generalization of eqs. (I.1.35) and (I.1.36) to the case of the double differential cross sections as expressed by the van Hove correlation functions can be achieved by considering two correlation functions. The first one gives rise to the coherent scattering by considering the correlation between all particles (summation over all pairs of atoms i and j) weighted by their coherent scattering length for each atomic species in the sample (i.e., averaged over all isotopes and nuclear spin states for each atomic species):

$$g_{\text{coh}}(\vec{r}, t) = \langle \bar{\rho}^*(\vec{R}, 0) \bar{\rho}(\vec{R} + \vec{r}, t) \rangle \quad \text{with} \quad \bar{\rho}(\vec{r}, t) = \sum_i \bar{b}_i \delta(r-r_i(t)), \quad (\text{I.1.37})$$

$$\left(\frac{d^2\sigma}{dE' d\Omega}\right)_{\text{coh}} = \frac{k'}{k} \int_V d\vec{r} \frac{1}{2\pi\hbar} \int_{-\infty}^{\infty} g_{\text{coh}}(\vec{r}, t) e^{-i(\vec{q}\vec{r}-\omega t)} dt = \frac{k'}{k} S_{\text{coh}}(\vec{q}, \omega). \quad (\text{I.1.38})$$

The second one corresponds to considering only the self-correlations of the atoms, that is, the correlation between the positions of the same atom at time $t=0$ and at an arbitrary time t , weighted by the incoherent scattering length for each atomic species (i.e., the root square deviation from the average for that atomic species):

$$g_{\text{self}}(\vec{r}, t) = \left\langle \sum_i \rho_i^{\text{inc}}(\vec{R}, 0) \rho_i^{\text{inc}}(\vec{R} + \vec{r}, t) \right\rangle \quad \text{with} \quad \rho_i^{\text{inc}}(\vec{r}, t) = b_i^{\text{inc}} \delta(r-r_i(t)), \quad (\text{I.1.39})$$

$$\left(\frac{d^2\sigma}{dE' d\Omega}\right)_{\text{inc}} = \frac{k'}{k} \int_V d\vec{r} \frac{1}{2\pi\hbar} \int_{-\infty}^{\infty} g_{\text{inc}}(\vec{r}, t) e^{-i(\vec{q}\vec{r}-\omega t)} dt = \frac{k'}{k} S_{\text{inc}}(\vec{q}, \omega). \quad (\text{I.1.40})$$

For mathematical completeness, note that the incoherent scattering length as defined in eq. (I.1.8) and given in the tables (<http://www.ncnr.nist.gov/resources/n-lengths/>) can only be a real, positive number.

The simplest example of a self-correlation function often encountered in soft matter is the one describing conventional diffusion of atoms, such as hydrogen, which can be readily observed by inelastic neutron scattering due to the high incoherent cross section of the proton. If a particle was found at $r=0$ at $t=0$, at a later time t its finding probability will be described by a Gaussian distribution around its original position with the mean square distance for displacement in the diffusion process linearly increasing with the time: $\sigma^2 \propto t$. Thus,

$$g_{\text{self}}(\vec{r}, t) \propto (b^{\text{inc}})^2 e^{-3r^2/2\sigma^2}. \quad (\text{I.1.41})$$

By Fourier transformation in the space variable r , we get the intermediate scattering function, which will also be a Gaussian function of the form $\exp(-q^2\sigma^2/6)$. Keeping in mind that $\sigma^2 \propto t$, we can rewrite the exponent here by introducing an appropriate proportionality constant D and we get

$$I_{\text{inc}}(\vec{q}, t) = (b^{\text{inc}})^2 e^{-q^2 D |t|}. \quad (\text{I.1.42})$$

This intermediate scattering function satisfies the requirement that at $t=0$ it has to be equal to the differential cross section $d\sigma/d\Omega$. The observation of this scattering function by NSE spectroscopy is an efficient way to study diffusion processes. In soft and glassy matter, one often finds unconventional “sublinear” diffusion, which implies that the mean square displacement evolves with time slower than linearly, that is, $\sigma^2 \propto t^\beta$, with $\beta < 1$. This leads in eq. (I.1.42) to the so-called stretched exponential form for the time dependence of the intermediate scattering function: $e^{-(t/\tau)^\beta}$ instead of the conventional $e^{-t/\tau}$, with τ being the characteristic time constant. By inspecting the right-hand side of eq. (I.1.42), we find that τ varies as q^{-2} in the case of conventional diffusion. In contrast, we find $\tau \propto q^{-2/\beta}$ for the unconventional sublinear diffusion.

The double differential cross section will be obtained by Fourier transformation of the intermediate scattering function in eq. (I.1.42) with respect to the time variable. This results in the well-known scattering function for the double differential inelastic cross section consisting of a Lorentzian line around zero energy transfer $\hbar\omega$ (the so-called quasielastic scattering):

$$S_{\text{inc}}(q, \omega) = \frac{(b^{\text{inc}})^2}{\pi} \frac{\Gamma^2}{\Gamma^2 + (\hbar\omega)^2}, \quad (\text{I.1.43})$$

where the full width at half maximum (FWHM) of the Lorentzian line is $\Gamma = Dq^2$. This behavior is the well-known signature of conventional diffusion processes, which is often explored by incoherent quasielastic neutron scattering.

We have obtained this result by using a classical mechanical picture of particle diffusion, which leads to the Gaussian correlation function, eq. (I.1.41). This is an excellent approximation at high sample temperatures, that is, for times t that are much longer than the characteristic time of thermal fluctuations given by the thermal energy $k_B T$ as $t_{\text{th}} = \hbar/k_B T$. In other terms, this condition will translate into the relation $\Gamma = Dq^2 \ll k_B T$.

I.1.12 DETAILED BALANCE, BOSE FACTOR

Inelastic neutron scattering involves energy changes of the neutron: either the incoming neutron transfers energy to the sample and loses energy in the scattering process or the neutron can take up energy from the sample in the scattering process and go out with an energy gain. The probabilities of both processes are exactly implied in the mathematical properties of the van Hove correlation functions. We will recall here two significant aspects, which are important quantum mechanical requirements. We will use plausibility arguments to introduce them.

The fundamental difference between classical and quantum notions of processes involving exchange of energy between objects is that quantum mechanics revealed that this exchange can happen only in quanta; that is, in a process with angular frequency ω , the energy change can only be a multiple of $E = \hbar\omega$. In the exchange of energy between the sample and the neutron, this becomes a prominent effect, when the thermal energy of the sample $k_B T$ is smaller than or comparable to $\hbar\omega$. Here k_B is the Boltzmann constant and T is the temperature. Since the thermal fluctuations provide the energy for the sample that can be communicated to the neutron, it takes a long time—that is, will become a process of lower probability—to wait for a thermal fluctuation that can deliver energy more than $k_B T$. Actually, this probability is known to be proportional to $\exp(-E/k_B T)$. This leads to an expression in the detailed balance property of the dynamic structure factor $S(\vec{q}, \omega)$:

$$S(\vec{q}, \omega) = e^{-\hbar\omega/k_B T} S(\vec{q}, -\omega), \quad (\text{I.1.44})$$

where $\omega > 0$ means energy gain for the neutron in the scattering and $\omega < 0$ means neutron energy loss. Mathematically, we also need to assume here that the reversal of the direction of \vec{q} has no effect on the sample (i.e., it is inherently microscopically symmetric), which generally holds for soft matter. This so-called detailed balance condition implies that the probability of the scattering process with neutron energy gain $E = \hbar\omega > 0$ is lower than that of the process with equal neutron energy loss (i.e., energy transferred to the sample) just by the thermal probability for the sample to be in a higher energy initial state by this amount.

Detailed balance is a very general requirement and it is exactly obeyed in nature, if the sample is in thermal equilibrium, that is, if it can be characterized by a unique temperature. Beyond spurious inhomogeneities of the sample temperature, there can

also be a physically founded breakdown of thermal equilibrium, if the temperature of one part of the system develops extremely long thermal equilibration times. A practical case of interest is the temperature of nuclear spin systems, which occasionally are very weakly coupled to the rest of the sample. A prominent case is molecular hydrogen, where the thermal equilibrium between the *ortho* and *para* states at low temperatures can take several days to be reached.

The other property of $S(\vec{q}, \omega)$ we will consider is related to the temperature dependence of the inelastic scattering probabilities. Let us assume, as an example, that the sample has a spectrum of excitations, which can be characterized by the density of states function $Z(\omega)$. It tells us how many excited states are between energy $\hbar\omega$ and $\hbar(\omega + \delta\omega)$, where by definition ω is positive. We can envisage the state of the system at a given temperature, by assuming that these excited states are occupied by a factor n , which is given by the Bose statistical occupation number

$$n = \frac{1}{e^{\hbar\omega/k_B T} - 1}, \quad (\text{I.1.45})$$

where by definition $\omega > 0$ must hold. For high temperatures, this expression becomes in good approximation $n = \hbar\omega/k_B T$. The probability for the neutron to gain $\hbar\omega$ energy in the scattering will be proportional to the occupation number n of the states with this energy. In contrast, the probability for the neutrons to lose energy (i.e., excite an excitation with energy $\hbar\omega$) is required by quantum mechanics to be $n + 1$. This is summarized by the Bose factor $n_B(\omega)$ for the temperature dependence of the cross section for neutron to scatter on this spectrum of excitation $Z(\omega)$:

$$n_B(\omega) = \begin{cases} n + 1, & \omega < 0, \\ n, & \omega > 0. \end{cases} \quad (\text{I.1.46})$$

It is to be stressed that the sign of ω here refers to the sign of the neutron energy change, and $|\omega|$ is to be used for the calculation of the occupation number n according to eq. (I.1.45). Note that with this definition $n_B(\omega)$ satisfies the detailed balance condition, eq. (I.1.44).

Measured scattering functions $S(\vec{q}, \omega)$ often show a temperature dependence proportional to $n_B(\omega)$, which suggest that indeed the sample displays a spectrum of excitations $Z(\omega)$, which itself is independent of the temperature, that is, only the occupation numbers change. Such a temperature dependence governed by the Bose factor is called harmonic. It indicates that the sample is in a robust state that in itself is little influenced by the temperature.

When the temperature dependence of $S(\vec{q}, \omega)$ cannot be accounted for by the Bose factor in eq. (I.1.46), it becomes “anharmonic.” This is an indication of changes of the state and functioning of the sample. Such anharmonic evolutions are frequent in soft matter and deserve particular attention. For example, the onset of diffusion (i.e., particles in the sample become mobile to move over substantial distances) is a process that typically does not obey Bose factor temperature dependence. It is rather controlled by the evolution of the diffusion constant D , cf. eq. (I.1.43), which can

follow Arrhenius-type activation instead. Indeed, the onset of diffusion indicates a substantial change in the function of the atoms: they do not stay anymore around an equilibrium position. Note that eq. (I.1.43) derived from a classical model obviously violates detailed balance, as all classical model calculations principally do, since the scattering function, eq. (I.1.43), is symmetric, the same for ω and $-\omega$. This is a good approximation if $k_{\text{B}}T \gg \hbar\omega$, which usually holds for the slow diffusion processes, and there are phenomenological approaches to reconcile classical model calculations with detailed balance (Squires, 1978).

REFERENCES

- KARDJILOV, N., FIORI, F., GIUNTA, G., HILGER, A., RUSTICHELLI, F., STROBL, M., BANHART, J., and TRIOLO, R. *J. Neutron Res.* **2006**, *14*, 29.
- MEZEL, F. and DAGLEISH, P.A. *Commun. Phys.* **1977**, *2*, 41.
- SQUIRES, G.L. *Introduction to the Theory of Thermal Neutron Scattering*, Cambridge University Press, Cambridge, 1978.
- van HOVE, L. *Phys. Rev.* **1954**, *95*, 249.